Supplement of Atmos. Chem. Phys., 22, 13449–13466, 2022
https://doi.org/10.5194/acp-22-13449-2022-supplement

Atmospheric Chemistry and Physics
Open Access
EGU

Supplement of

Hygroscopicity and CCN potential of DMS-derived aerosol particles

Bernadette Rosati et al.

Correspondence to: Bernadette Rosati (bernadette.rosati@chem.au.dk) and Merete Bilde (bilde@chem.au.dk)

- Example of selection of limits for the main growth-mode
- Schematic of SMCA calibration of CCNc and calibration curve of the instrument
- DMS decay rates at dry and humid conditions at temperatures of 293, 273 and 258 K
- OH radical concentration estimation from 1-butanol decay experiments
- Size dependence of κ-values
- Bulk particle relative chemical composition from HR-ToF-MS
- Hygroscopicity parameter κ for Exp. 8 and 10 at 273 and 258 K
- Tabular values of mean GF(80%) values from nano- and long-HTDMA
- Tabular values of mean κ-values, supersaturations and critical diameters from CCNc
- HR-ToF-MS organic signal from Exp. 5
- MSA to sulphate ratios from HR-ToF-MS
- Hydration free energy and hydrate distributions
- Bibliography

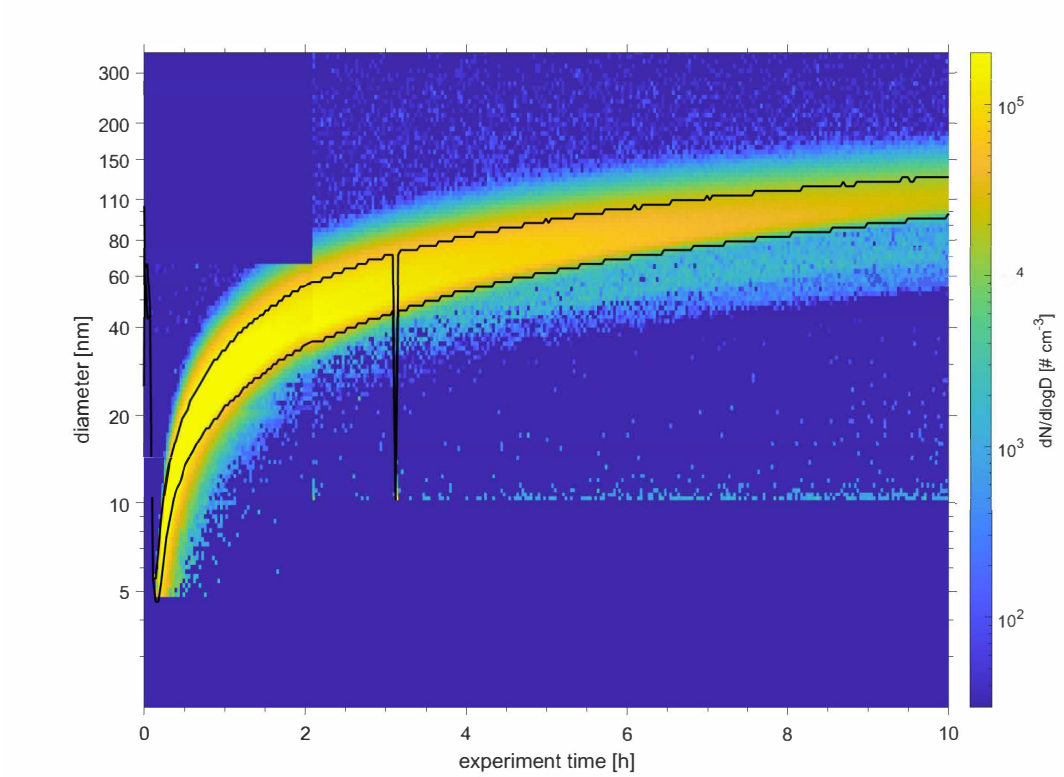

Figure S1: Example of selection of limits for the main growth-mode. Data from Exp.5 (26.2.2019 - experiment at 293 K).

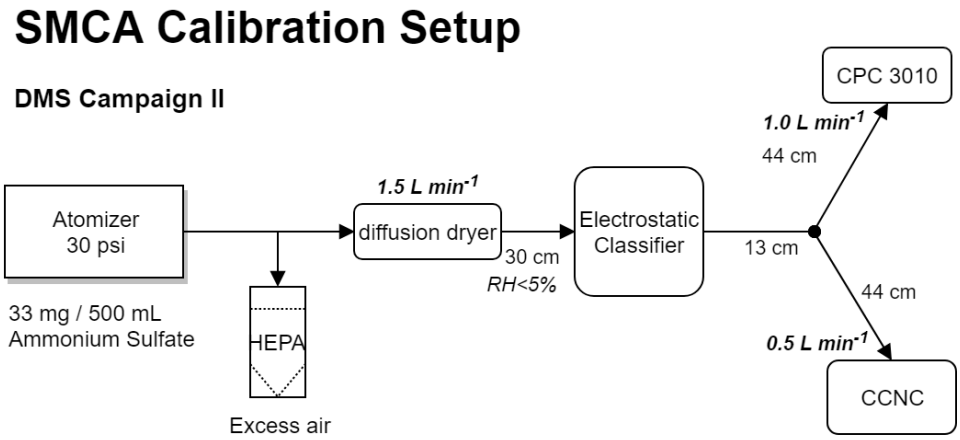

Figure S2: Setup when calibrating the CCN counter.

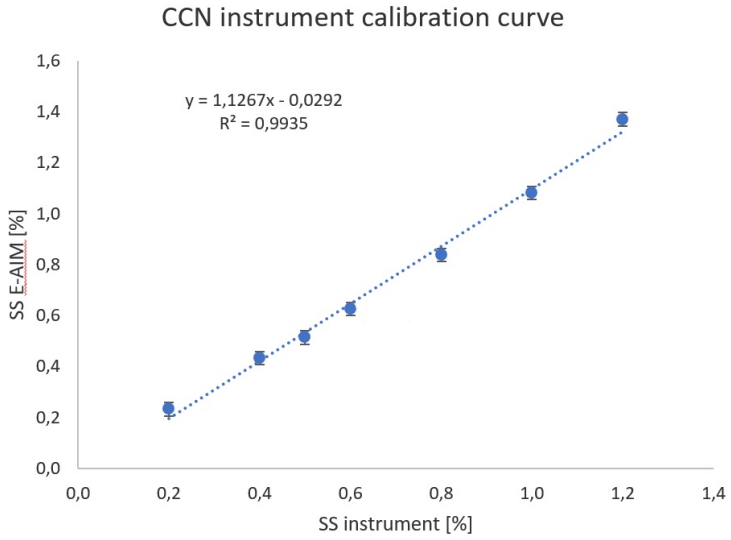

Figure S3: CCN instrument calibration curve.

DMS decay rates

DMS decay rates measured with the PTR-MS during Exp. 1 (previously presented in Rosati et al.[1]), 2, 8 and 10 are shown in Fig. S4. These experiments were chosen to give an example for each temperature probed during this work and both dry and humid conditions. The data were fitted using a first order fit, assuming constant OH concentration and thus pseudo-first-order conditions. Table S1 summarises the derived rate constants for the loss of DMS from fits of the change in DMS concentrations over time compared to the DMS initial concentration (DMS_0).

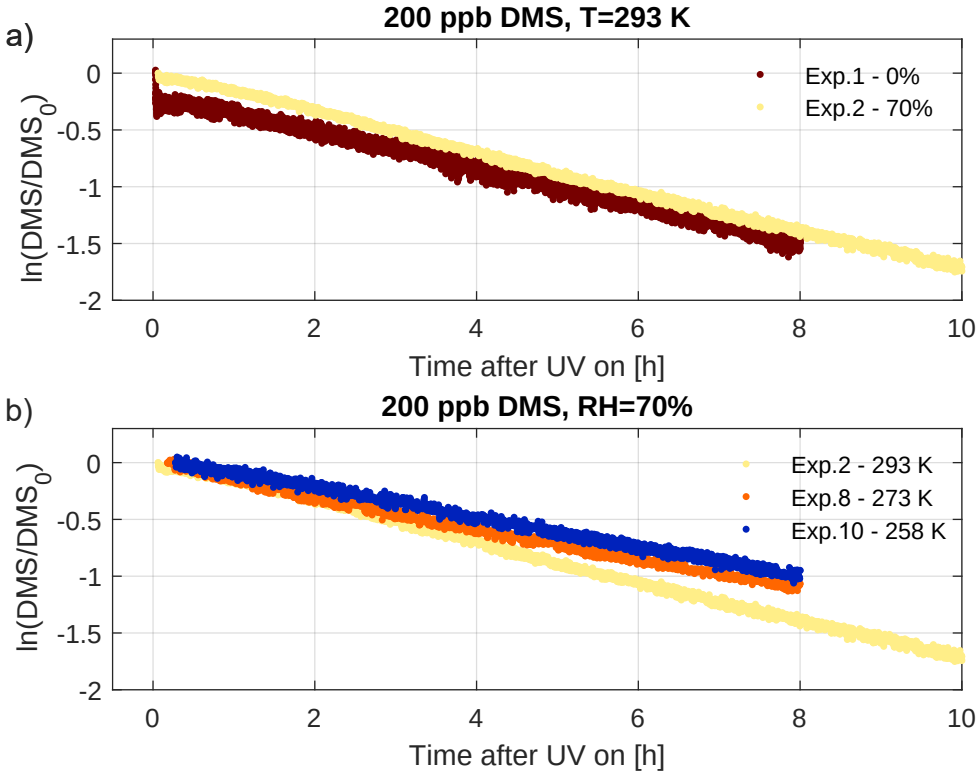

Figure S4: DMS decay rates: a) for dry (RH=0%) and humid (RH=70%) conditions at T=293 K (Exp. 1 vs. 2), b) at different temperatures and humid conditions (Exp. 2, 8, 10).

Table S1: Rate constants for the reaction of DMS with OH radicals as derived from first order fits to the data seen in Fig.S4. $k_{DMS,exp}$ denotes the slope of the fit of $\ln(DMS/DMS_0)$, $\Delta k_{DMS,exp}$ the uncertainty (1σ) in the slope and R^2 the goodness of the fit. T and RH denote the values set in the AURA chamber, see Table 1 in main manuscript for actual values.

Exp. #	DMS [ppb]	T [K]	RH [%]	$k_{DMS,exp}$ [s^{-1}]	$\Delta k_{DMS,exp}$ [s^{-1}]	R^2
Exp. 1	200	293	0	-4.43e-05	1.37e-06	0.99
Exp. 2	200	293	70	-4.84e-05	1.57e-06	0.99
Exp. 4	400	293	70	-5.02e-05	2.81e-06	0.99
Exp. 5	400	293	70	-4.87e-05	2.75e-06	0.99
Exp. 8	200	273	70	-3.84e-05	3.80e-06	0.99
Exp. 9	400	273	70	-3.41e-05	6.21e-06	0.99
Exp. 10	200	258	70	-3.64e-05	3.75e-06	0.99
Exp. 11	400	258	70	-3.18e-05	6.22e-06	0.98

OH radical estimation

Three experiments were performed to estimate OH radical concentrations. A detailed description of the experimental procedure of the 1-butanol experiments can be found in the SI of Rosati et al. (2021a)[1]. Figure S5 illustrates the loss of 1-butanol as measured with a gas chromatography flame ionisation detector (GC-FID) with time, while Table S2 presents the slopes of linear least squares fit to the experimental data and derived OH concentrations. The conditions during the 3 1-butanol experiments are representative for the conditions during the DMS-experiments presented in this paper covering temperatures of 293 K, 273 K and 258 K and high humidity conditions.

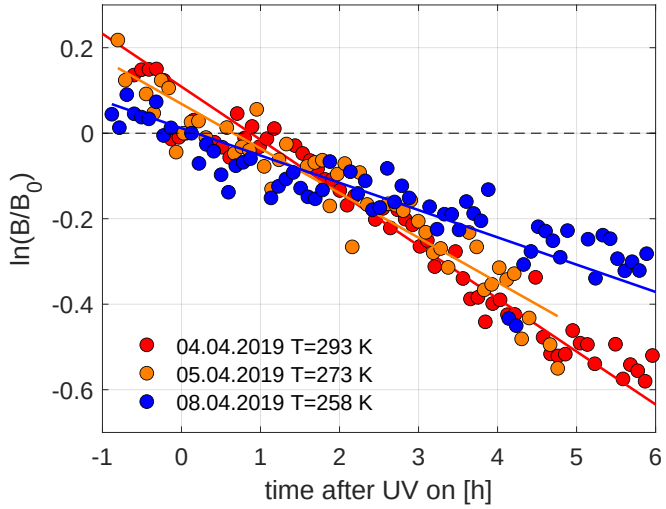

Figure S5: 1-butanol decay rates: Experiments were carried out at humid conditions and temperatures of 293 K, 273 K and 258 K, respectively, and using an initial concentration of 1.5 mL H_2O_2. Lines denote the fit to the data points (spheres).

Table S2: Fitting results for 1-butanol decay rates illustrated in Fig. S5: A first order fit was assumed. k_{exp} denotes the slope of a linear least squares fit to the experimental data, $\Delta k_{b,exp}$ the uncertainty of the fit (1σ) and R^2 the goodness of the fit. T and RH denote the temperature and relative humidity during the experiments in the AURA chamber. The OH concentration was derived using a temperature dependent rate constant for the reaction of OH radicals with 1-butanol of $k = 5.30 \cdot 10^{-12}$ exp(146/T) cm^3 $molecules^{-1}s^{-1}$ according to Yujing et al.[2].

Date	T [K]	RH [%]	$k_{b,exp}$ [s^{-1}]	$\Delta k_{b,exp}$ [s^{-1}]	R^2	OH [molecules/cm^3]
04.04.2019	293	40-55	-3.44e-05	3.70e-05	0.97	3.94e+06
05.04.2019	273	70-80	-2.90e-05	1.02e-04	0.88	3.20e+06
08.04.2019	258	80	-1.77e-05	2.94e-05	0.92	1.90e+06

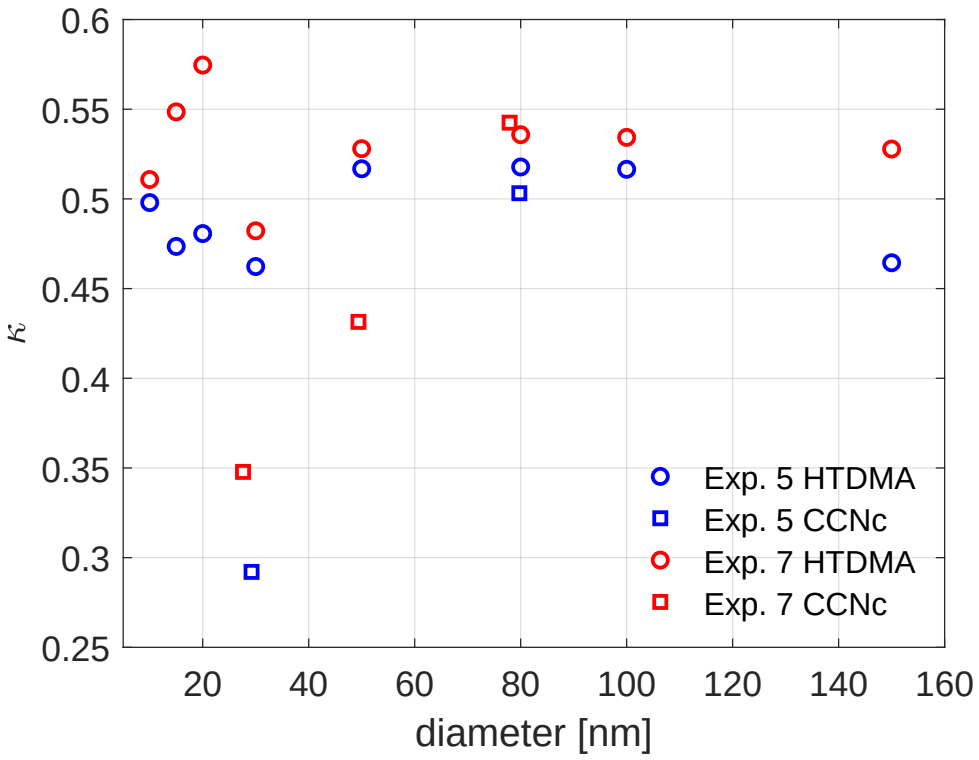

Figure S6: Size dependent κ-values as derived from measurements during Exp. 5 (humid, T=293K) and 7 (dry, T=293K). Spheres denote results from HTDMA measurements (both nano- and long-HTMDA) and squares from CCNc.

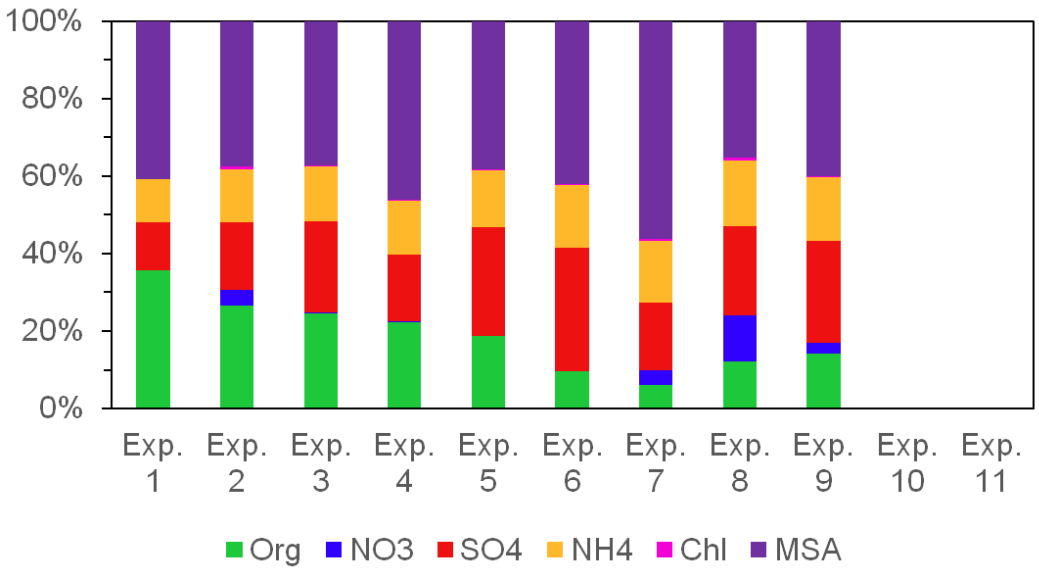

(a) Relative mass concentrations.

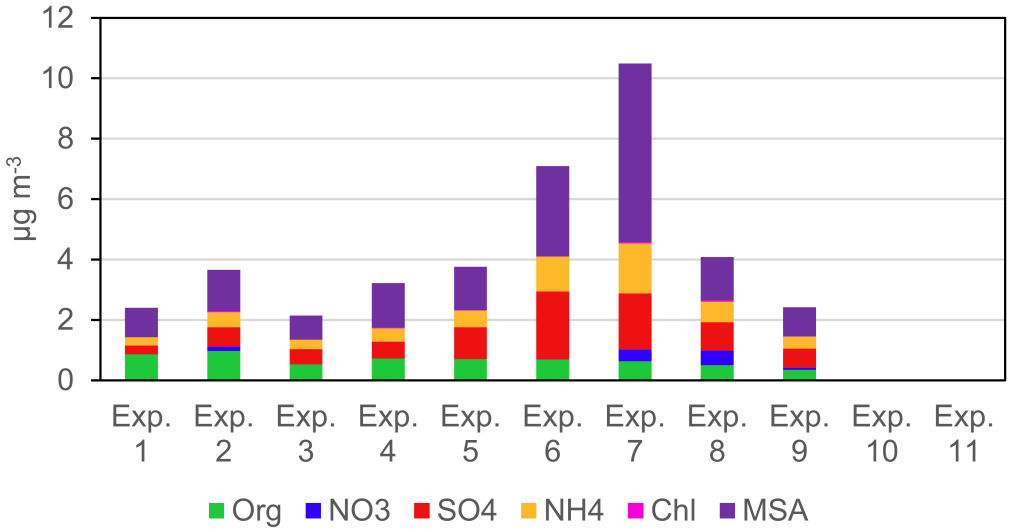

(b) Absolute mass concentrations.

Figure S7: HR-ToF-AMS-measured particle composition: organics, NO_3^-, SO_4^{2-}, NH_4^+, chloride, and MSA are shown. Results for Exp. 1, 6 and 7 were previously presented in Rosati et al.[(1)] and are included here for completeness.

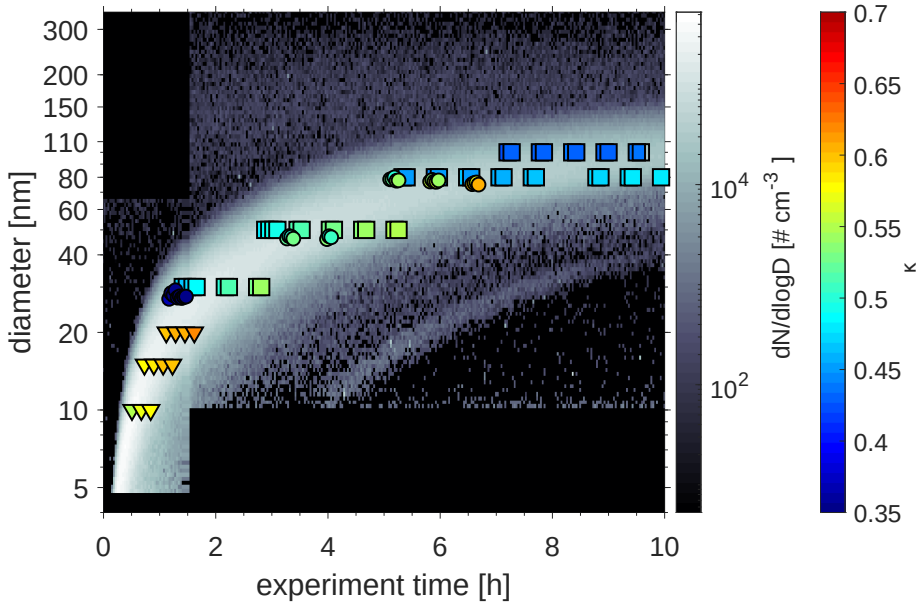

Figure S8: Exp. 8 at 273 K. κ values as calculated from nano- (triangles) and long-HTDMA (squares) for different dry sizes are shown together with results from the CCNc (circle).

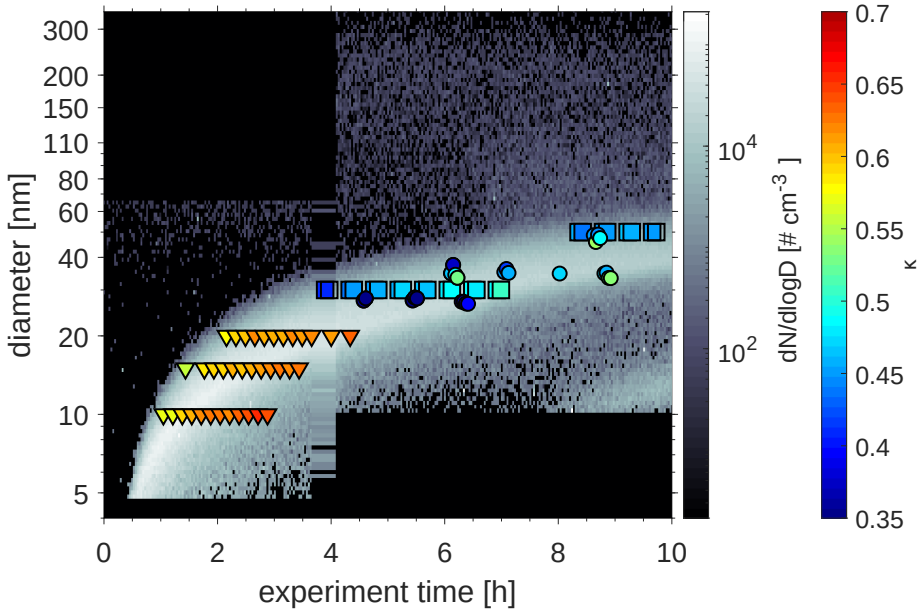

Figure S9: Exp. 10 at 258 K. κ values as calculated from nano- (triangles) and long-HTDMA (squares) for different dry sizes are shown together with results from the CCNc (circle).

Table S3: Mean GF(80%) values and their standard deviations (sd) as calculated from nano- and long-HTDMA.

	D_{dry} = 10 nm		D_{dry} = 15 nm		D_{dry} = 20 nm		D_{dry} = 30 nm		D_{dry} = 50 nm		D_{dry} = 80 nm		D_{dry} = 100 nm		D_{dry} = 150 nm	
Exp. #	mean	sd	mean	sd	mean	sd	mean	sd	mean	sd	mean	sd	mean	sd	mean	sd
1	1.26	0.00	1.30	0.02	1.34	0.02	1.36	0.02	1.40	0.02			1.39	0.01	1.36	0.00
2	1.23	0.01	1.30	0.01	1.34	0.02	1.34	0.04	1.36	0.03			1.39	0.01	1.38	0.00
3	1.27	0.01	1.30	0.02	1.34	0.01	1.32	0.03	1.38	0.02	1.40	0.02	1.40	0.01		
4	1.23		1.28	0.02	1.32	0.03	1.33	0.04	1.38	0.03	1.41	0.02	1.42	0.02	1.39	0.01
5	1.27		1.30	0.01	1.33	0.01	1.35	0.04	1.41	0.03	1.42	0.02	1.43	0.02	1.40	0.01
6	1.28	0.01	1.34	0.01	1.38	0.01										
7	1.27	0.01	1.34	0.01	1.38	0.02	1.36	0.02	1.41	0.03	1.44	0.02	1.44	0.02	1.44	0.02
8	1.29	0.02	1.36	0.01	1.39	0.01	1.35	0.03	1.40	0.02	1.38	0.02	1.38	0.01		
9	1.30	0.00	1.35	0.01	1.40	0.01	1.39	0.02	1.42	0.00	1.44	0.02	1.44	0.01		
10	1.31	0.01	1.37	0.01	1.40	0.01	1.38	0.03	1.40	0.02						
11	1.35	0.01	1.40	0.01	1.43	0.01	1.38	0.02								

Table S4: Mean κ-values and their standard deviations (sd) as calculated from the supersaturations (SS) and critical diameters ($D_{p,c}$) measured in the CCNc.

	D_{dry} [nm]		SS [%]	κ		D_{dry} [nm]		SS [%]	κ		D_{dry} [nm]		SS [%]	κ	
Exp. #	mean	sd		mean	sd	mean	sd		mean	sd	mean	sd		mean	sd
1	27.27	1.20	1.37	0.36	0.05	48.49	0.95	0.51	0.46	0.03	85.33	2.08	0.23	0.41	0.03
2	30.25	0.36	1.37	0.26	0.01	48.50	5.35	0.51	0.40	0.03	81.71	1.60	0.23	0.47	0.03
3															
4	28.88	0.58	1.37	0.30	0.02	48.67	1.29	0.51	0.45	0.04	80.10	10.48	0.23	0.46	0.04
5	29.22	0.79	1.37	0.29	0.02						79.75	1.41	0.23	0.50	0.03
6	27.43	0.80	1.37	0.36	0.03	47.98	1.28	0.51	0.47	0.04	77.57	3.09	0.23	0.55	0.07
7	27.61	0.70	1.37	0.35	0.03	49.39	0.82	0.51	0.43	0.02	77.91	2.74	0.23	0.54	0.06
8	27.25	1.04	1.37	0.36	0.04	47.44	1.27	0.51	0.49	0.04	77.29	1.36	0.23	0.55	0.03
9	27.04	0.81	1.37	0.37	0.04	47.70	0.92	0.51	0.48	0.03	76.97	2.10	0.23	0.56	0.05
10	29.66	3.82	1.37	0.39	0.06	41.12	6.11	0.51	0.50	0.05					
11	26.59	0.88	1.37	0.39	0.04										

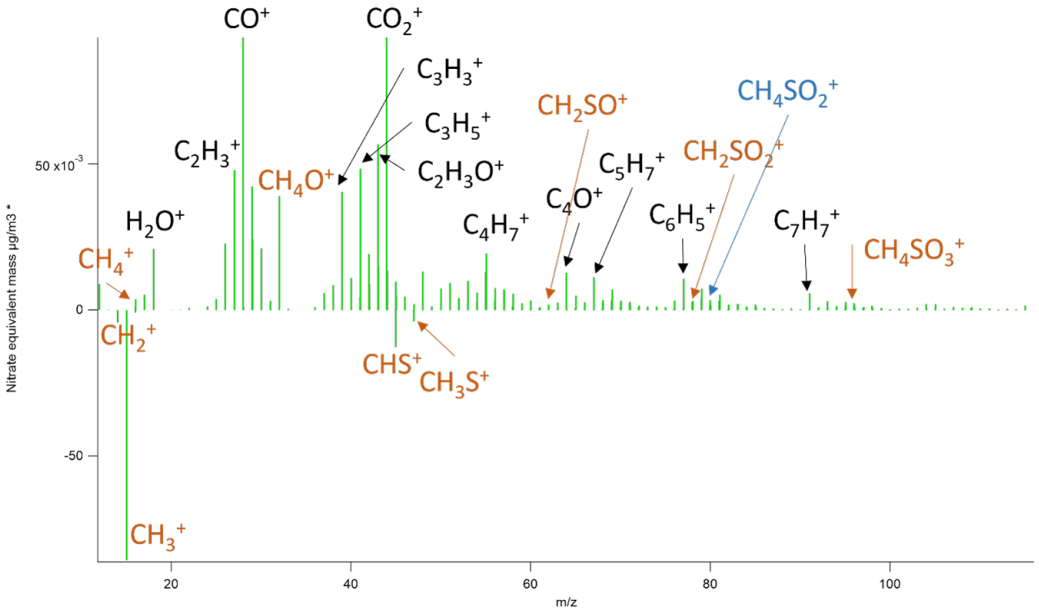

Figure S10: High resolution mass spectrum of the organic signal measured during the time period where the particle mass peaked in Exp. 5. The ions indicated in orange color denote ions also found during the MSA calibration. Ions denoted in black color have an unknown origin. The ion denoted in blue could stem from MSIA.

Table S5: MSA to sulphate ratios as measured by the HR-ToF-MS. T and RH denote the values set in the AURA chamber, see Table 1 in main manuscript for actual values. At 258 K (Exp. 10 and 11) the particle mass was too low to achieve a good measurement of the chemical composition.

Exp. #	DMS [ppb]	T [K]	RH [%]	MSA/SO_4
Exp. 1	200	293	0	3.3
Exp. 2	200	293	70	2.2
Exp. 3	200	293	70	1.6
Exp. 4	400	293	70	2.7
Exp. 5	400	293	70	1.4
Exp. 6	400	293	0	1.3
Exp. 7	400	293	0	3.2
Exp. 8	200	273	70	1.5
Exp. 9	400	273	70	1.5
Exp. 10	200	258	70	–
Exp. 11	400	258	70	–

S1 Hydration Free Energy and Hydrate Distributions

The step-wise reaction free energies for adding the n'th water molecule to a cluster can be calculated as:

$$\Delta G_{\text{water,add}} = \Delta G_n - \Delta G_{n-1}$$

The stepwise reaction free energy ($\Delta G_{\text{water,add}}$) for the $(MSA)_1(H_2O)_{1-5}$ clusters are shown in Table S6 compared to the $(SA)_1(H_2O)_{1-5}$. The data for sulphuric acid - water clusters are taken from[3]. All the calculations are at the DLPNO-CCSD(T)/aug-cc-pVTZ//ωB97X-D/6-31++G(d,p) level of theory, at 298.15 K and 1 atm. Figure S11 shows the hydrate distributions of MSA at 20%, 40%, 60%, 80% and 100% relative humidity.

Table S6: Stepwise reaction free energy ($\Delta G_{\text{water,add}}$ in kcal/mol) for adding water molecules to the $(MSA)_1(H_2O)_{1-5}$ clusters. Calculated at 298.15 K and 1 atm.

n	SA	MSA
1	-1.7	-1.0
2	-1.0	-0.3
3	-1.1	-0.6
4	-1.1	1.1
5	1.6	-0.2

The reaction free energy for adding the first four water molecules to MSA seem to be less favourable than adding water molecules to sulphuric acid. This indicates that gas phase MSA is significantly less hygroscopic compared to SA.

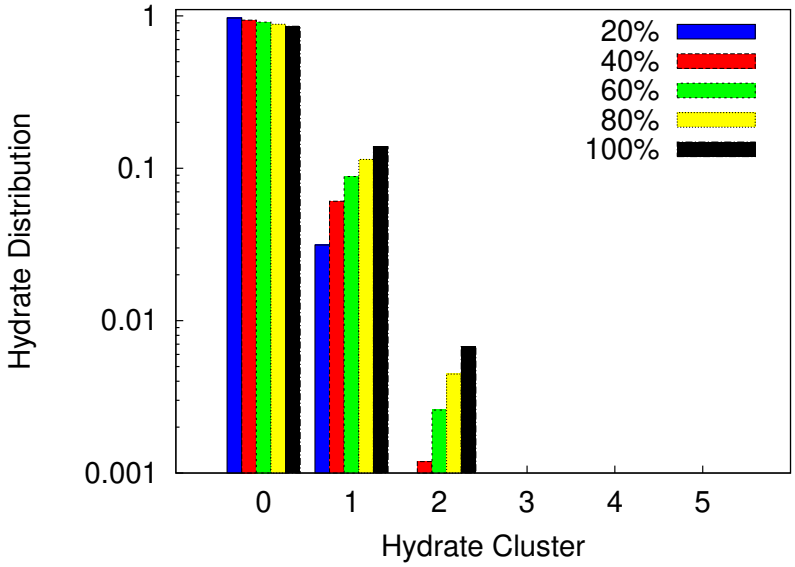

Figure S11: Calculated hydrate distribution of the MSA - water clusters. The calculations are performed at the DLPNO-CCSD(T)/aug-cc-pVTZ//ωB97X-D/6-31++G(d,p) level of theory, at 298.15 K and 1 atm.

Bibliography

[1] Bernadette Rosati, Sigurd Christiansen, Robin Wollesen de Jonge, Pontus Roldin, Mads Mørk Jensen, Kai Wang, Shamjad P. Moosakutty, Ditte Thomsen, Camilla Salomonsen, Noora Hyttinen, Jonas Elm, Anders Feilberg, Marianne Glasius, and Merete Bilde. New particle formation and growth from dimethyl sulfide oxidation by hydroxyl radicals. *ACS Earth and Space Chemistry*, 5(4):801–811, 2021a.

[2] Mu Yujing and Abdelwahid Mellouki. Temperature dependence for the rate constants of the reaction of oh radicals with selected alcohols. *Chemical Physics Letters*, 333(1):63 – 68, 2001.

[3] J. V. Kildgaard, K. V. Mikkelsen, M. Bilde, and J. Elm. Hydration of atmospheric molecular clusters: A new method for systematic configurational sampling. *J. Phys. Chem. A*, 122:5026–5036, 2018.